Geminate Ion Kinetics for Hexa-, Penta- and Tetrachloroethane in Liquid Methylcyclohexane (MCH): Effect of the Anion Lifetimes

M. A. Quadir,[†] T. Azuma,[‡] A. S. Domazou,[§] Y. Katsumura,[||] and R. E. Bühler*

Laboratory for Physical Chemistry, ETH Zürich, Switzerland

Received: April 18, 2003; In Final Form: September 29, 2003

We have previously shown that, in the case of extremely short lived chlorocarbon anions (of CCl_4, $CFCl_3$) in liquid MCH solutions, one observes the formation and decay of the solvent separated ion pairs $(R^+||Cl^-)_{solv}$, instead of the geminate ion recombination between the solvent cation (MCH^+) and the fragment anion (Cl^-). For longer lived anions ($CHCl_3^-$) there was no formation of ion pairs (IPs) observable. To evaluate the correlation between IP formation and anion lifetime τ^-, three new chlorocarbon solutes (RCl), hexachloroethane (Hexa), pentachloroethane (Penta), and tetrachloroethane (Tetra), were studied, for which a coarse lifetime classification from positronium studies suggested that $Hexa^-$ and $Penta^-$ should be short lived (IP formation possible) and $Tetra^-$ long lived (no IP formation). The results in this paper agree with this expectation and confirm the correlation with τ^-. With anion lifetimes of 250 and 150 ns for $Hexa^-$ and $Penta^-$ at 143 K, ion pairs were observed, whereas $Tetra^-$ with $\tau^- = 13.7$ μs decayed too late to yield IPs. The solvent separated ion pairs are formed through charge transfer (CT) from MCH^+ to the fragment radical $R^\bullet$ from the anion decay: $MCH^+ + R\bullet\cdot\cdot Cl^- - \eta \rightarrow (R^+||Cl^-)_{solv}$. The IP absorption is due to the CT band of ($R^+ \leftarrow$ MCH), and the stability relates to the complexing with the solvent. The efficiency η for CT reduces with time and therefore correlates to the anion lifetime: the later $R^\bullet$ is freed, the lower η. It also correlates with the ratio of D_{fast}/D_{diff} (competition of the high mobility approach of MCH^+ (with D_{fast}) toward Cl^- and the diffusional escape of $R^\bullet$ (with D_{diff}), away from Cl^-). It is shown that η reduces by a factor of about 6 from 133 to 295 K in parallel to D_{fast}/D_{diff} reducing from 400 to 10. It is concluded that the high mobility of the solvent cation is a requirement for positive CT from MCH^+ to $R^\bullet$. The IP formation therefore gains importance at very low temperature; however, it loses importance at room temperature. The IP lifetime at 143 K is longest for CCl_4 ($\tau_{ip} = 111$ μs), followed by Hexa ($\tau_{ip} = 22.7$ μs) and Penta ($\tau_{ip} = 5.3$ μs). If no IP is detectable, IP formation is still possible, but $\tau_{ip} \ll \tau^-$ (probably true for $CHCl_3$). For all IPs so far found (list of 7 given) the IP decay rate constant k_{ip} is characterized by a very low preexponential Arrhenius factor of $\log A \approx 8-10$. For CCl_4, Hexa, and Penta, the $\log A$ values are 9.0 ± 0.2, 8.3 ± 0.3, and 10.4 ± 0.4, respectively. Simulation of the complete mechanism is rather complex, but it is carefully analyzed with schemes of various complexity, particularily with and without the cation mechanism, related to the precursor M^{+*} of the high mobility cation MCH^+. It is shown that the details of the cationic mechanism are covered up by the strong absorption from the ion pair IP, if formed.

I. Introduction

In the past we have reported on the geminate ion kinetics for some chlorocarbons in liquid methylcyclohexane (MCH), studied by pulse radiolysis, mostly at low temperatures. The solutes were CCl_4,[1−3] $CFCl_3$,[4] and $CHCl_3$.[5] They all scavenge electrons (e^-_{solv}) to form anions, which then fragment by a variety of rates. Consequentially, the geminate ion kinetics is built up of three consecutive pairs of geminate ions, as shown in Scheme 1. The initial step of electron scavenging usually was outside of the observation time.

SCHEME 1

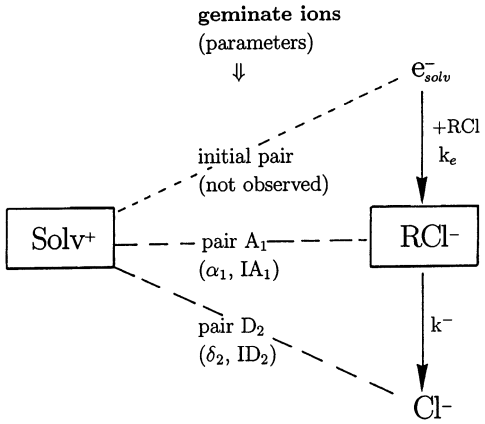

For $CHCl_3$[5] the anion fragmentation $CHCl_3^- \rightarrow CHCl_2^\bullet + Cl^-$ was directly observed as an overlap with the geminate

* To whom correspondence should be addressed. Mailing address: Physical Chemistry, ETH Zürich, Mühlebachstrasse 96, 8008 Zürich, Switzerland. Telephone: +41-1-383 16 13. Fax: +41-1-383 06 88. E-mail: buehler@phys.chem.ethz.ch.

† Present address: L'Oreal USA, Applied Research, 285 Terminal Ave, Clark, NJ 07066, USA.

‡ Present address: Dept of Physics, Tokyo Metropolitan University, 1-1-1 Minami-Osawa, Hachioji, Tokyo 192-0397, Japan.

§ Present address: Laboratory for Inorganic Chemistry, ETH Zürich, Hönggerberg, 8093 Zürich, Switzerland.

|| Nuclear Engineering Research Laboratory, School of Engineering, University of Tokyo, Shirakata Shirane 2-22, Tokai-mura, Ibaraki 319-1106, Japan.

10.1021/jp030481j CCC: $25.00
Published on Web 12/03/2003

SCHEME 2

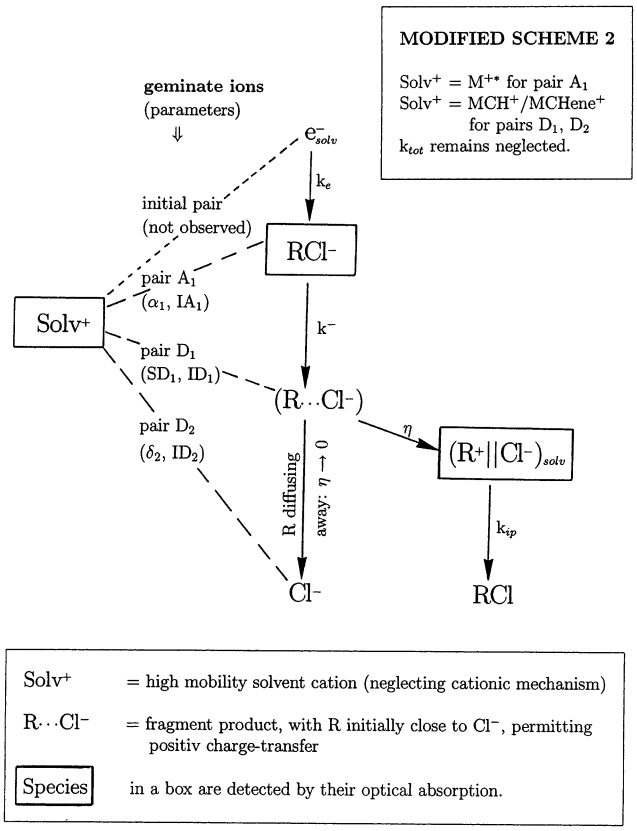

recombination kinetics, revealing a fragmentation rate constant of $k^-(143\ \mathrm{K}) = 3.6 \times 10^6\ \mathrm{s}^{-1}$ (lifetime $\tau^- = 280$ ns).

CCl_4[1-3] and $CFCl_3$,[4] however, are characterized by extremely short lived anions. They appear to fragment within a single vibrational period, so that the geminate ion recombination should only be observed with the fragment anion Cl^-, very comparable to the findings with N_2O^- in a N_2O saturated solution in MCH.[1,6,7] However, a very strong absorption was found instead ($\lambda_{max} = 470$ nm), decaying by first order and covering up all expected geminate ion recombination kinetics. We have shown[1-3] that a product, absorbing at 470 nm, was formed from the geminate ion recombination: $Solv^+ + Cl^- \rightarrow$ Product, and the observed first-order decay is due to the decay of the geminate product. Scheme 2 illustrates the principle of the mechanism with CCl_4 or $CFCl_3$, where k^- is so rapid that the recombination of the primary pair of ions (A_1) is not observable. The crucial point of this mechanism is that the high mobility solvent cation is able to reach the anion Cl^- before the radical $R^\bullet$, from the anion dissociation, has time to diffuse away (visualized by writing ($R^\bullet \cdot\cdot Cl^-$)). Consequently, some of the cations ($Solv^+$) will find $R^\bullet$ (e.g. $CCl_3^\bullet$) available for positive charge transfer (CT) before reaching the anion. As shown in Scheme 2, the geminate ion recombination then ocurs between R^+ and Cl^-. The recombination product is a solvent separated ion pair $(R^+|MCH|Cl^-)_{solv}$ (or simply $(R^+||Cl^-)_{solv}$), stabilized by complexing with the solvent (or solute) molecule, thereby suppressing the neutralization for the length of the ion pair's lifetime. The absorption of this ion pair product was found to be due to the CT band between R^+ and MCH (or solute): $R^+ \leftarrow$ MCH.

There is a finite efficiency η with which such positive charge transfer ($Solv^+ + R^\bullet \rightarrow R^+$) may occur. Details of η are so far not known. However, η is expected to depend on how early $R^\bullet$ becomes available from the anion fragmentation. Short anion lives (e.g. CCl_4^- (ref 1)) lead to a high yield. For long anion lifetimes (e.g. $CHCl_3^-$ (ref 5)) $R^\bullet$ becomes available too late and the geminate kinetics follows Scheme 1.

The aim of this paper is to further evaluate the correlation with the anion lifetime. Therefore, experiments were chosen with anions expected to show different lifetimes. Unfortunately, there is little information about such lifetimes in the literature. From positronium (Ps) studies a very coarse classification of anion lifetimes was published,[8] which was based on the findings that Ps formation is suppressed by short anion lifetimes.[8] The anions of CCl_4, pentachloroethane (Penta), and hexachloroethane (Hexa) are classified as "short lived", whereas the anions of $CHCl_3$, CH_2Cl_2, and tetrachloroethane (Tetra) are called "long lived". In analogy it is expected that Penta and Hexa should also yield solvent separated ion pairs with a corresponding unimolecular decay, whereas Tetra should not. The results for these three chloroethanes are given in this paper.

Our method to analyze such ion kinetics is again based on the semiempirical $t^{-0.6}$ kinetic law[9] (see section III), which we extended to cover ion−molecule reactions and unimolecular ionic processes.

II. Experimental Section

A. Methods. The technique of pulse radiolysis with a Febetron 705 accelerator (Physics International) for 30 ns pulses of 2 MeV electrons has been used as reported.[6,7] Experiments with methylcyclohexane (MCH) as solvent were typically performed in the temperature range from 133 to 183 K in the liquid state. The stainless steel cell had an optical path length of 2 cm. A typical dose was between 50 and 120 Gy. Dosimetry was done by calorimetry. All data are normalized to 100 Gy, unless otherwise stated. The data treatment, kinetic analysis, and data simulation were based on a modified version of Tek-SPS-Basic from Tektronix. In the $t^{-0.6}$ linearity tests there are usually three different experimental curves from a single photomultiplier (Hamamatsu R1509). They cover three different, partially overlapping time ranges and are from two different transient digitizers: Tektronix 7912AD or 2440 and Datalab DL912. The experimental curves are partly smoothed by digital filtering.

All the experimental signals were corrected for the cell window signal (quartz defects).[6] The origin of shock waves in pulse radiolysis cells and the method to minimize the effect have also previously been discussed in detail.[6,10]

Room temperature pulse radiolysis was done at Tokai-mura (University of Tokyo)[11] with a LINAC for 28 MeV electrons, having a time resolution of 2 ns. The detection system was composed of a Hamamatsu R1328U-02 photodiode (rise time 60 ps) and a Tektronix SCD1000 transient digitizer (rise time 350 ps). Signal averaging was done on a NEC computer. For dosimetry a N_2O saturated aqueous solution of 10 mM KSCN was used. $(SCN)_2^-$ was observed at 472 nm with $G = 6.1$ (100 eV)$^{-1}$ and $\epsilon = 7580\ \mathrm{M}^{-1}\ \mathrm{cm}^{-1}$.[12]

B. Chemicals. Methylcyclohexane (MCH) (Fluka purum, >98% GC) was passed through a column of aluminum oxide, dried over molecular sieves A4, and then fractionated through a Fischer "Spaltrohrkolonne" with about 30 theoretical plates. Hexachloroethane (Hexa, C_2Cl_6), pentachloroethane (Penta, C_2HCl_5), 1,1,1,2-tetrachloroethane (1112-Tetra, CCl_3CH_2Cl), and 1,1,2,2-tetrachloroethane (1122-Tetra, $CHCl_2CHCl_2$) from Aldrich (>99%) and N_2O from PanGas, Luzerne CH (99%), were used as received.

III. Theory for Data Analysis

The simulation of the rate data is based on the semiempirical $t^{-0.6}$ kinetic law for the geminate ion recombination as initiated

by van den Ende et al.[13] It describes the probability of survival of the geminately recombining ions relative to the free ion yield:

$$\frac{G(t)}{G_{fi}} = 1 + \alpha t^{-0.6} = \frac{\text{absorbance}(t)}{\text{absorbance}(\infty)} = \frac{A(t)}{\text{IA}} \quad \text{with} \quad \alpha = 0.6\left[\frac{r_c^2}{D}\right]^{0.6} \quad (1)$$

where α is the mobility value and IA = $A(\infty)$ is the free ion intercept.

The absorption may have contributions from both types of ions (sum of both absorption coefficients). Any plot of the absorbance $A(t)$ against $t^{-0.6}$ should be linear. Its intercept IA for $t = \infty$ ($t^{-0.6} = 0$) corresponds to the absorbance of the free ion yield. The slope divided by the intercept IA is called α, a mobility value (or β, γ, etc. for other geminate pairs). From this value, with the known Onsager radius r_c, an experimental diffusion constant can be derived: $D_{exp} = D^+ + D^-$.

Theoretical support for the $t^{-0.6}$ rate law was given by Barczak and Hummel.[14,15] We have given experimental support [1,5−7,9,16−18] and could derive some experience about the validity range: for low-temperature studies in liquid MCH (e.g. 143 K) the $t^{-0.6}$ kinetic law holds at least to $t^{-0.6} = 4.0$ ($t \geqslant 100$ ns). In this range all deviations from the $t^{-0.6}$ linearity had a chemical reason and could be explained. For this purpose the theory was extended to cover such ionic reactions overlapping with the geminate ion recombination kinetics (for a survey, see ref 9).

A. If one ion reacts (ion−molecule reaction or unimolecular process with rate constant k_1), there is a change from a primary to a secondary pair of geminate ions that can be simulated by eqs 2−4.[6]

The primary geminate ion kinetics is given by

$$\frac{A_{prim}(t)}{\text{IA}} = [1 + \alpha t^{-0.6}]e^{-k_1 t} \quad \text{with} \quad \alpha = 0.6\left[\frac{r_c^2}{D_{prim}}\right]^{0.6} \quad \text{and} \quad \text{IA} = A_{prim}(\infty) \quad (2)$$

The secondary geminate ion kinetics is approximated by

$$\frac{A_{sec}(t)}{\text{IB}} = [1 + \beta t^{-0.6}][1 - e^{-k_1 t}] \quad \text{with} \quad \beta = 0.6\left[\frac{r_c^2}{D_{sec}}\right]^{0.6} \quad \text{and} \quad \text{IB} = A_{sec}(\infty) \quad (3)$$

The sum of primary and secondary ion absorbances then simulates the experimental time profile

$$A(t) = A_{prim}(t) + A_{sec}(t) \quad (4)$$

Application of this $t^{-0.6}$ simulation has been shown, for example, for positive charge scavenging with norbornadiene (NBD), $MCH^+ + NBD \rightarrow NBD^+$ (ref 6), or for anion fragmentation with chloroform, $CHCl_3^- \rightarrow Cl^- + CHCl_2^{\bullet}$.[5]

B. If one of the ions takes part in two parallel, competitive reactions, then the secondary geminate ions are mixed, possibly with different mobilities: for example, if the initial cation A^+ suffers simultaneously a fragmentation with k_c to yield C^+ and a relaxation with k_b to yield B^+, then the secondary cations (B^+ and C^+) are mixed. The decay rate for A^+ is $k_{tot} = k_b + k_c$. The mixed pairs are still following the $t^{-0.6}$ kinetics, even if the mobilities of the two product ions (mobility values β and γ) should differ.[5]

$$A_{tot} = \text{ID}[1 + \delta t^{-0.6}] \quad (5)$$

$$\delta = b\cdot\beta + (1 - b)\gamma \quad \text{with} \quad b = \left[1 + \frac{k_c}{k_b}\frac{(\epsilon_C^+ + \epsilon^-)}{(\epsilon_B^+ + \epsilon^-)}\right]^{-1} \quad (6)$$

$$\text{and an intercept of} \quad \text{ID} = G_{fi}(lf)\left[\epsilon^- + \frac{k_b}{k_{tot}}\epsilon_B^+ + \frac{k_c}{k_{tot}}\epsilon_C^+\right] \quad (7)$$

with f = [conc(M)/G value](1/100 eV) ≈ density (g·cm^{-3}) × dose (Gy) × 10^{-7} and l = optical cell length (cm).

In consequence, the effective mobility value δ for the mixed cations is higher than that for the high mobility ion alone and is λ dependent through the absorption coefficients ϵ_B^+, ϵ_C^+, and ϵ^-. For an application, see the paper on $CHCl_3$.[5]

C. If the product of a geminate ion recombination is an optical absorber ($\epsilon_p > 0$) in the λ range studied, then the intercept of the $t^{-0.6}$ linear plot is not just the free ion yield but, due to $\epsilon_p > 0$ and the large G_{tot} value, corresponds to a higher value and the slope is much lower (may even be negative):[1]

$$A(t) = \text{slope} \times t^{-0.6} + \text{intercept} \quad (8)$$

$$\text{slope} = \text{SX} = G_{fi}(lf)(\epsilon^+ + \epsilon^- - \epsilon_p)\alpha \quad (9)$$

$$\text{intercept} = \text{IX} = G_{fi}(lf)(\epsilon^+ + \epsilon^-) + (G_{tot} - G_{fi})(lf)\epsilon_p \quad (10)$$

In this case the quotient slope/intercept does not yield the mobility value. For an application of this result, see the formation of the solvent separated ion pair $(CCl_3^+||Cl^-)_{solv}$ from $CCl_3^+ + Cl^-$ in a solution of CCl_4 in MCH.[1]

D. If mixed ions (e.g. B^+, C^+) recombine with a common counterion (e.g. X^-) to form products (e.g. P_B, P_C), both with optical absorbances (ϵ_{pb}, ϵ_{pc}), then the calculation follows the same procedure as that needed for case C; however, the two parallel recombinations (e.g. $B^+ + X^- \rightarrow P_B$ and $C^+ + X^- \rightarrow P_C$) enter with their fractions $f_b = k_b/k_{tot}$ and $f_c = k_c/k_{tot}$. The corresponding absorption coefficients are ϵ_B^+, ϵ_C^+ for the mixed ions and ϵ_{pb}, ϵ_{pc} for the products, and the corresponding mobility values are β, γ. The total absorbance still follows eq 8:

$$A(t) = \text{slope} \times t^{-0.6} + \text{intercept}$$

$$\text{slope} = \text{SX} = G_{fi}(lf)[f_b(\epsilon_B^+ + \epsilon^- - \epsilon_{pb})\beta + f_c(\epsilon_C^+ + \epsilon^- - \epsilon_{pc})\gamma] \quad (11)$$

$$\text{intercept} = \text{IX} = G_{fi}(lf)[f_b\epsilon_B^+ + f_c\epsilon_C^+ + \epsilon^-] + (G_{tot} - G_{fi})(lf)[f_b\epsilon_{pb} + f_c\epsilon_{pc}] \quad (12)$$

In this case the quotient slope/intercept does not yield the mobility value. An application follows in this paper.

E. If there are two consecutive ionic reactions, covering different time ranges, then the simulation of the individual reaction steps may be added to simulate the total rate curve. For an application, see the results for the MCH solution of quadricyclane.[17]

F. If both positive and negative ions suffer independent reactions, then the two separate simulations may be added. However, for successful treatment, the corresponding time ranges should be different. For an application, see the results in this paper.

IV. The Three Systems in Comparison

A. The transient spectra for the three chlorocarbons in MCH solution at 143 K are shown in Figure 1, and the spectral data

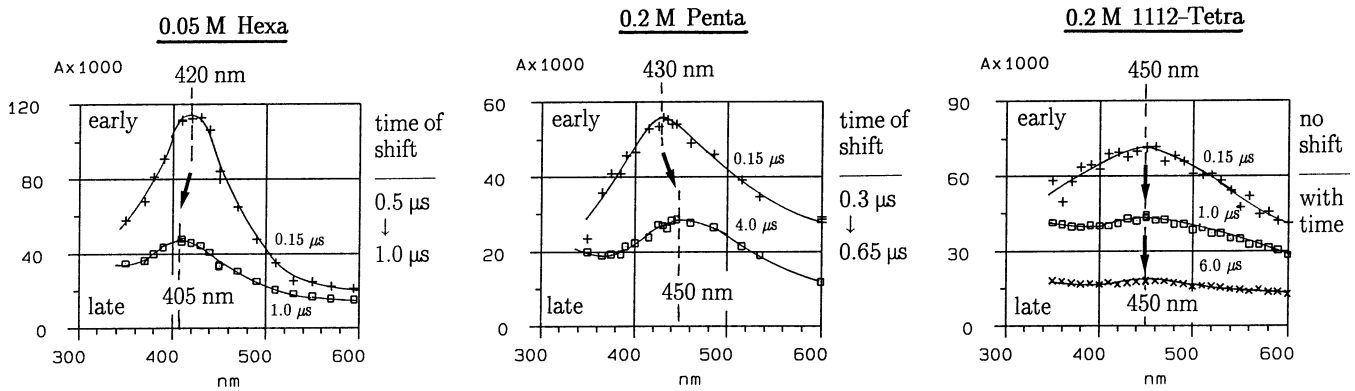

Figure 1. Transient spectra for the three chlorocarbons in MCH solution at 143 K, normalized to 100 Gy, as a function of time. Spectral details at other temperatures are given in Table 1.

TABLE 1: Spectral Data for the Transients

		λ_{max}/nm		λ shift (early → late)	
system	*T*/K	early	late	$\Delta\lambda$/nm	time of shift/μs
Hexa (0.05 M)	143	420	405	−15	0.5 → 1.0
Penta (0.2 M)	133	430	470	+40	0.25 → 8.0
	143	430	450	+20	0.35 → 0.65
	295		430		
1112-Tetra (0.2 M)	133	450	450	0	
	143	450	450	0	
1122-Tetra (0.2 M)	143	430	430	0	

are summarized in Table 1. The transient spectra for Hexa and Penta reveal a band shift with time near about 1 μs, indicating that the early transient is different from the later one. Contrary to this, the Tetra system is not showing any band shift: neither at 143 K nor at 133 K, for neither of the two isomers studied, 1112-Tetra and 1122-Tetra.

B. For Hexa and Penta the characteristics of the early and late transients are different: Hexa has a shift of −15 nm, yet Penta has one at 143 K of +20 nm (at 133 K even +40 nm). Furthermore, for Penta the early λ_{max} is temperature independent, whereas the late λ_{max} strongly varies with *T*. These differences basically correspond to the expected mechanism: The early transient is compatible with the solute anion, showing an internal, unaffectable optical transition. The late transient may be assigned to the expected solvent separated ion pair $(R^+||Cl^-)_{solv}$ with a charge-transfer band (CT band) of R^+ with a solvent molecule. CT bands are known to critically depend on the solvent condition.

C. For Tetra a single transient absorption is observed, with no apparent band shift with temperature. In analogy to the early transient with Hexa and Penta, it is reasonable to assign the Tetra transient to the expected anion $Tetra^-$ (for both isomers).

D. The large kinetic differences for the three solutes can be seen in Figure 7. The rate curve for Hexa is the most surprising one: two decay segments are separated by a plateaulike region, which happens to correspond to the time range of the λ_{max} shift. The details of Hexa therefore are discussed first.

V. Hexachloroethane (Hexa)

A. Scheme 2 is taken as the most simple mechanism to explain the geminate kinetics in a solution of Hexa in MCH, as shown with a $t^{-0.6}$ plot in Figure 2a. It assumes a single, high mobility solvent cation $Solv^+$ and neglects the details of the cationic mechanism, as they appear of minor importance relative to the dominant absorptions of the negative species.

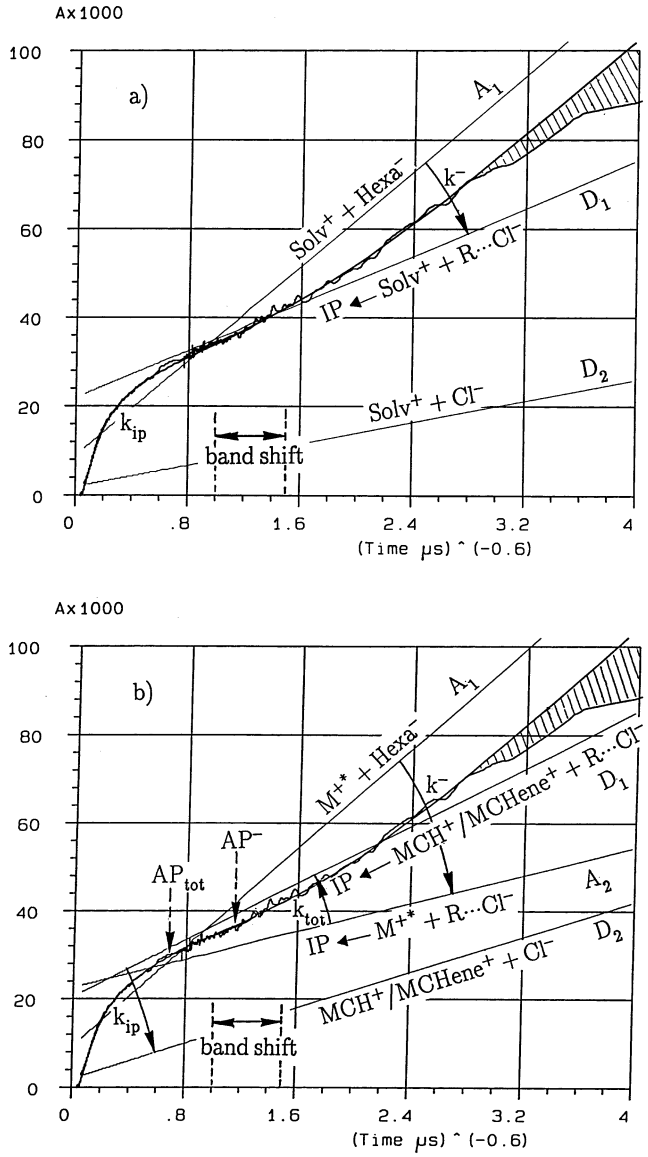

Figure 2. Hexachloroethane: $t^{-0.6}$ plot of the rate curve for 0.05 M Hexa in MCH at 143 K and 450 nm (normalized to 100 Gy). Part a represents the simulation based on Scheme 2. Part b illustrates the simulation with Scheme 3 (including the cationic mechanism). AP_{tot} and AP^- mark the positions of the anchor points for k_{tot} and k^- for 5% rest.[20] For parts a and b the parameters are given in Table 2. The hatched area marks the deviation due to $Hexa^-$ buildup from electron scavenging ($AP_e(1\%) = 2.7$).

TABLE 2: Hexachloroethane (0.05 M): Kinetic Parameters for the Rate Analysis in Figure 2 (143 K, 450 nm, and Normalized to 100 Gy)

geminate lines →		A_1			A_2			D_1			D_2	
reactions →		M^{+*} or $Solv^+$ + $Hexa^-$		$Hexa^-$ decay	$M^{+*} + R\cdot\cdot\cdot Cl^- \rightarrow IP$		M^{+*} decay	$MCH^+/MCHene^{+\,b}$ + $R\cdot\cdot\cdot Cl^- \rightarrow IP$		IP decay	$MCH^+/MCHene^{+b}$ + Cl^- (final)	
comments ↓	schemes ↓	α_1 $\mu s^{0.6}$	$IA_1/10^{-3}$	$k^-/10^6$ s^{-1}	$SA_2/10^{-3}$ $\mu s^{0.6}$	$IA_2/10^{-3}$	$k_{tot}/10^6$ s^{-1}	$SD_1/10^{-3}$ $\mu s^{0.6}$	$ID_1/10^{-3}$	$k_{ip}/10^3$ s^{-1}	δ_2 $\mu s^{0.6}$	$ID_2/10^{-3}$
Figure 2a	2	3.0	8.9	4.0				13.31	22.0	42	3	2.0
	2 mod	3.0	8.9	4.0				13.31	22.0	44	5	2.0
Figure 2b	3	3.0	9.4	4.0	7.95	22.7	1.6[19]	16.19	20.6	42	5	2.0
mean[a]	2 mod	3.0	8.5 ± 0.5	4.0 ± 0.3				13.13 ± 0.85	21.8 ± 1.4	44.8 ± 5.8	5	2.0

[a] Mean of 12 rate curves, all parameters dose independent from 42 to 250 Gy. [b] For Scheme 2 the cation is $Solv^+$.

TABLE 3: Hexachloroethane (0.05 M): Temperature Dependence of the Kinetic Parameters for the Modified Scheme 2 (430 nm, Normalized to 100 Gy)

geminate lines →	A_1			D_1			D_2	
reactions →	M^{+*} + $Hexa^-$		$Hexa^-$ decay	$MCH^+/MCHene^+ + R\cdot\cdot\cdot Cl^- \rightarrow IP$		IP decay	$MCH^+/MCHene^+$ + Cl^-	
temp K	α_1 $\mu s^{0.6}$	$IA_1/10^{-3}$	$k^-/10^6$ s^{-1}	$SD_1/10^{-3}$ $\mu s^{0.6}$	$ID_1/10^{-3}$	$k_{ip}/10^3$ s^{-1}	δ_2 $\mu s^{0.6}$	$ID_2/10^{-3}$
143	3.0	11.3 ± 0.5	4.0 ± 0.3	13.0 ± 0.8	32.0 ± 2.0	44 ± 5	5.0	2.0
153	2.0	7.7 ± 0.4	9.7 ± 0.3	6.1 ± 0.7	26.1 ± 0.6	90 ± 10	3.3	2.0
163				5.3 ± 0.3	22.2 ± 0.2	152 ± 12	2.5	2.0
173				4.1 ± 0.2	19.5 ± 1.0	240 ± 19	1.0	2.0
183				3.1 ± 0.4	18.0 ± 0.5	310 ± 25	1.5	2.0

As the early spectrum is due to the anion $Hexa^-$ (section IV), the initial decay corresponds to the anion fragmentation $Hexa^- \rightarrow R\cdot\cdot\cdot Cl^-$ (with $R{=}C_2Cl_5$), or rather to the change from the primary geminate pair A_1 ($Solv^+ + Hexa^-$) to the secondary pair D_1 ($Solv^+ + R\cdot\cdot\cdot Cl^-$), corresponding to Scheme 2. The recombination kinetics of the secondary pair D_1 fits to the plateau region, with a $t^{-0.6}$ linearity of low slope and high intercept. The latter makes clear that a product is formed with an optical absorbance (section III.C). In analogy to the findings with CCl_4 in MCH,[1-3] the recombination product is expected to correspond to the solvent separated ion pair $(R^+||Cl^-)_{solv}$, as a result of the preceding positive charge transfer from $Solv^+$ to the fragment radical $R^\bullet$ (efficiency η). The optical absorption of $(R^+||Cl^-)_{solv}$ then is again assigned to the CT band between R^+ and a solvent molecule[2] within the ion pair. The first-order decay then corresponds to the collapse of the solvent separated ion pair $(R^+||Cl^-)_{solv} \rightarrow RCl$, leading to the final geminate recombination of the secondary pair D_2 ($Solv^+ + Cl^-$). At late times the efficiency η for charge transfer is expected to reach zero. For details, see the Discussion.

B. The simulation with Scheme 2 (excluding electron scavenging) is shown in Figure 2a, and the corresponding data of the simulation are given in Table 3. The fit with two consecutive reactions (section III.E) is surprisingly good, even though the cationic mechanism has been neglected and a single high mobility cation $Solv^+$ has been assumed. There are two aspects to be mentioned:

(1) For hexachloroethane *the ion pair decay reaches into the time of free ion recombination* (at 143 K typically $t^{-0.6} \lesssim 0.15$ $\mu s^{-0.6}$). The final geminate line D_2 ($Solv^+/Cl^-$) therefore crosses the experimental curve. The corresponding δ_2 and ID_2 were taken from previous results: $ID_2(450\ nm) = 2.0 \times 10^{-3}$ (calculated from the known $\epsilon(MCH^+)$[4]) and $\delta_2 = 3.0$ $\mu s^{0.6}$ (for the high mobility cation $Solv^+$ (ref 6)).

(2) For the low concentration 50 mM Hexa *the anion buildup from electron scavenging* reaches into the early part of the observation time. With $k_e = 4.8 \times 10^8$ M^{-1} s^{-1} (ref 19) the corresponding anchor point (1% rest of electron scavenging)[20] is $AP_e = 2.7$ $\mu s^{-0.6}$. This explains the deviation from the simulated curve for $t^{-0.6} > 2.7$ $\mu s^{-0.6}$ as seen in Figure 2 (hatched area).

SCHEME 3

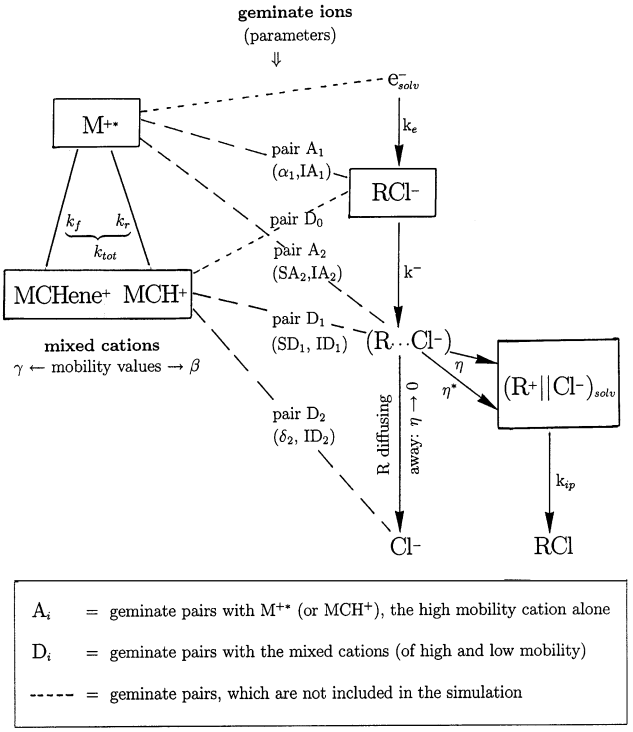

In reality we know that there is a *cationic mechanism*,[7] *as shown in Scheme 3*: a high mobility precursor M^{+*} fragments into methylcyclohexene$^+$ ($MCHene^+$) and relaxes simultaneously to the high mobility cation MCH^+. The secondary cations form a mixed pair of geminate ions (see section III.B).

In the following an attempt to analyze the kinetics of this rather complex Scheme 3 is given. The aim is to judge the accuracy of the data derived from the more simple Scheme 2, particularly concerning the rate constants k^- and k_{ip}.

The cationic mechanism with $k_{tot} = k_f + k_r$ and $k_r = k_0 + k_2$ [RCl] cannot be derived from these experiments. One has to rely on previous data with other solutes, like $CHCl_3$[5] or tetrachloroethane (see adjacent paper[19]), which, however, differ to some extent. Both sets of data have been used for the simulation, with almost no difference. The results from Tetra[19] were chosen to explain the simulation: $k_{tot} = 1.6 \times 10^6\ \mu s^{-1}$ with $k_r/k_f = 6.6$, $k_2 = 0$ (no dependence on [RCl]), and $\delta_2 = 5.0\ \mu s^{0.6}$ for the mixed pairs.

The geminate pair D_0 is ignored, as $Hexa^-$ fragments faster than k_{tot} and as there are no further criteria available to test on such a contribution.

C. The procedure of simulation with Scheme 3 then starts as usual with the latest time (ion pair decay) and continues to the earliest part (anion decay); see Figure 2b and Table 2.

Step 1. The ion pair decay kinetics is fitted between the geminate line D_1 and D_2, in the region where k_{tot} has no more influence, which means for $t^{-0.6} < AP_{tot}(5\%)$ (anchor point[20] for k_{tot} with 5% rest). The parameters are the slope and intercept (SD_1 and ID_1) of the geminate line D_1 and k_{ip} for the decay of the ion pair (IP). The geminate line D_1 is slightly steeper than that as derived from Scheme 2 (see Table 2), because the next simulation step pulls the curve downward.

Step 2. Starting from the fitted geminate line D_1, the preceding geminate line A_2 is searched from theory by comparing eqs 10 and 12 for the intercept and eqs 9 and 11 for the slopes. All ϵ (except for the products) are known, as are the mobility values α, β, and γ and the ratios f_b and f_c. The term with G_{tot} is dominating as $G_{tot} \gg G_{fi}$, and the two $\epsilon_{pi} = \eta_i \epsilon_{ip}$ for the products differ only by the differences of η_i, which are judged to correspond to $\eta(MCHene^+) \ll \eta(MCH^+) \approx \eta(M^{+*})$, due to their mobilities. On that basis the intercept for the M^{+*} geminate line (A_2) should be about 10% higher than that for the line (D_1), and the slope must be smaller (because $\epsilon(M^{+*}) < \epsilon(MCH^+)$[7]). Consequently, with the estimated higher intercept, the slope is lowered so that a fit in the time window from $AP_{tot}(5\%)$ to $AP^-(5\%)$ is reached.

Step 3. The anion decay (with k^-) must now be fitted between the geminate lines A_1 (parameter IA_1 with $\alpha_1 = 3.0\ \mu s^{0.6}$) and A_2 from step 2 for $t^{-0.6} > AP^-$.

D. The complete procedure is illustrated in Figure 2b for a typical experiment, with parameters given in Table 2 for comparison with the results from Scheme 2. The resulting rate constants, k^- and k_{ip}, derived with Schemes 2 and 3 are the same within experimental error limits. It is therefore permissible to simulate by neglecting the cationic mechanism.

For the ultimate simulation, Scheme 2 was slightly modified by replacing $Solv^+$ by the mixed cations (MCH^+,$MCHene^+$) for the last geminate line (D_2), which increased the mobility value to $\delta_2 = 5.0\ \mu s^{0.6}$.[19] The effect of this is a slight increase for k_{ip} (see Table 2), which is judged the best value.

E. All final simulations were now based on the modified Scheme 2, with $Solv^+ = M^{+*}$ for the geminate lines A_1 and A_2 and with $Solv^+ =$ mixed cations for the geminate lines D_1 and D_2 (k_{tot} being neglected). The result from 12 different experimental rate curves is given as mean data in Table 2. They are independent of dose from 42 to 250 Gy. The rate constant for the $Hexa^-$ fragmentation is k^- (143 K) = (4.0 ± 0.3) × 10^6 s^{-1}. The decay rate of the solvent separated ion pair $(R^+||Cl^-)_{solv}$ is k_{ip}(143 K) = (4.5 ± 0.6) × 10^4 s^{-1}.

F. The temperature dependence of all parameters in the range 143−183 K is given in Table 3, and the Arrhenius results are shown in Figure 3. For k_{ip} (the decay of the late transient) there is a very low preexponential value of log *A*. This is again

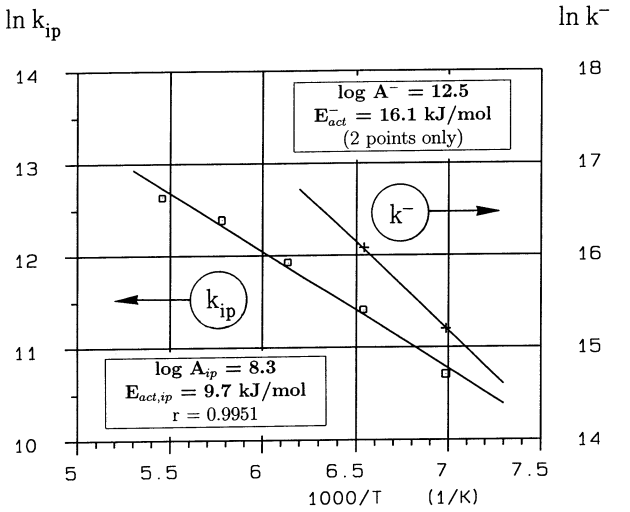

Figure 3. Hexachloroethane: Arrhenius plots for the rate constants k^- (anion fragmentation) and k_{ip} (decay of solvent separated ion pairs, IP), including the Arrhenius parameters for the data as summarized in Table 3.

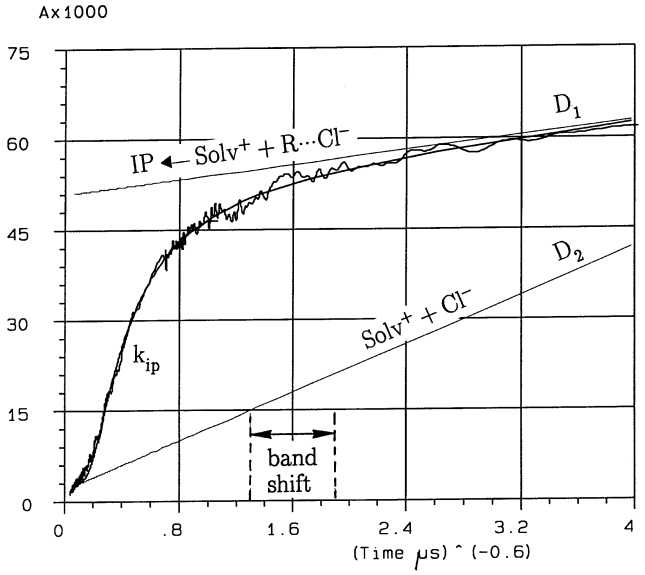

Figure 4. Pentachloroethane: $t^{-0.6}$ plot of the rate curve for 0.1 M Penta in MCH at 143 K and 450 nm (normalized to 100 Gy) with the simulation on the basis of the modified Scheme 2. The parameters are given in the first line of Table 4.

support for the assignment to the solvent separated ion pair, as previously found for $(CCl_3^+||Cl^-)_{solv}$ in MCH solutions of CCl_4.[2]

The intercept ID_1 (Table 3) is also strongly temperature dependent. From 143 to 183 K the value for $ID_1 \times 10^3$ drops from 32 to 18. This reflects a yield reduction of solvent separated ion pairs (IPs) toward higher temperature and is correlated with the loss of efficiency η for charge transfer (compare with the detailed analysis of ID_1 in the discussion on Penta, next section).

VI. Pentachloroethane (Penta)

For spectral reasons (section IV) and in analogy to the case of Hexa, it is expected that the early transients at $t^{-0.6} > 1.9\ \mu s^{-0.6}$ with $\lambda_{max} = 430$ nm are due to the anion $Penta^-$ (RCl^-) and the late one at $t^{-0.6} < 1.3\ \mu s^{-0.6}$ with $\lambda_{max} = 450-470$ nm (Table 1) is due to a solvent separated ion pair $(R^+||Cl^-)_{solv}$ with $R = C_2HCl_4$.

A. The early anion decay is not directly observable (Figure 4). However, from the time of the band shift (disappearance of

TABLE 4: Pentachloroethane (0.1 M): Temperature Dependence of the Kinetic Parameters for the Modified Scheme 2 (Normalized to 100 Gy)

geminate lines →			D_1			D_2		
reactions →			$MCH^+/ene^+ + R\cdots Cl^- \rightarrow IP$		IP decay	$MCH^+/ene^+ + Cl^-$		
temp K	no. exp averaged	λ nm	$SD_1/10^{-3}$ $\mu s^{0.6}$	$ID_1/10^{-3}$	$k_{ip}/10^3$ s^{-1}	δ_2 $\mu s^{0.6}$	$ID_2/10^{-3}$	comments
143		450	3.0	51	190	5.0	2.0	details for Figure 4
133	7	450	2.4 ± 1.0	67 ± 2.6	71.5 ± 1.3	7.5	2.0	indep of dose from 35 to 300 Gy
143	9	450	3.0 ± 0.2	50.2 ± 2.3	187 ± 15	5.0	2.0	indep of dose from 35 to 300 Gy
143	9	var	*a*	*b*	190 ± 15	*a*	2.0	transient spectra
143	7	450	3.2 ± 0.9	36.0 ± 0.9	191 ± 12	5.0	2.0	N_2O sat. (ID_1: −28%)
153	4	450	2.5 ± 0.3	38.8 ± 0.5	455 ± 19	3.3	2.0	indep of dose from 80 to 350 Gy
163	4	450	3.3 ± 0.4	29.3 ± 0.9	790 ± 14	2.5	2.0	indep of dose from 90 to 380 Gy
295	8	var	0.36 ± 0.01[c]	20.0 ± 0.4[b,c]	$83\,000 \pm 9\,000$	0.145 [5]	2.0	exp in Tokai mura, Japan

[a] λ dependent. [b] See Figure 5. [c] Data from $\lambda_{max} = 430$ nm only.

the early transient) the lifetime of the anion may be estimated. The mean time of the λ shift is $t^{-0.6} \approx 1.6\ \mu s^{-0.6}$ (Table 1). It is expected to correspond to the anchor point[20] of the early decay for about 5% rest: $AP^-(5\%) = 1.6\ \mu s^{-0.6}$. This allows us to derive the anion decay rate constant to be $k^- \approx 7 \times 10^6\ s^{-1}$. The reason that this decay is not seen in Figure 4 may be due to the $Penta^-$ disappearance being faster than that for $Hexa^-$ and due to the fact that there is still an overlap with the cationic mechanism, as discussed for Hexa. Therefore, the tail of the anion decay is partly compensated by the increase from the cationic absorption (compare with Figure 2b for Hexa).

Consequently, the simulation for $t^{-0.6} > 1.6\ \mu s^{-0.6}$ is hampered and the apparent good fit for the upper geminate line (D_1) is not so perfect as it looks in Figure 4. Yet, the uncertainty affects the slope SD_1 only; the intercept ID_1 is quite reliable.

B. The late decay after the band shift ($t^{-0.6} < 1.6\ \mu s^{-0.6}$) is simulated by a flat geminate line D_1 with high intercept (formation of $(R^+||Cl^-)_{solv}$) and a first-order decay of $(R^+||Cl^-)_{solv}$ to the final geminate line D_2 ($Solv^+ + Cl^-$), as described by the modified Scheme 2. The high intercept of the upper geminate line (D_1) is representative for the total yield of $(R^+||Cl^-)_{solv}$ (see below: analysis of SD_1 and ID_1). The first-order rate constant is k_{ip}. The simulation of the ion pair decay is shown in Figure 4 for a typical rate curve, and the corresponding parameters are given in the first line of Table 4. The other data in Table 4 are mean values for various temperatures and conditions.

In all low-temperature systems the parameters did not show any dose effects (dose variation by a factor of 8−9). N_2O, however, reduced the yield of ion pairs (ID_1) by −28%, as expected for the solvated electron being precursor. There was no effect on the kinetics. Particularly, k_{ip} remains unaffected.

The spectral studies (375 nm $\leqslant \lambda \leqslant$ 525 nm) show that k_{ip} is independent of λ, proof that a single transient is observed. The intercept spectra ID_1 for 143 and 295 K are shown in Figure 5. They correspond to the late spectra in Figure 1 (compare with λ_{max} in Table 1).

C. The temperature effect on the rate constant k_{ip} is seen in Table 4 and is shown as an Arrhenius plot in Figure 6. The activation energy for k_{ip} is $E_{act} = 14.1 \pm 1.1$ kJ/mol, and the preexponential factor is $\log A = 10.4 \pm 0.4$. As expected, the preexponential factor is again low, which is characteristic for all of the solvent separated ion pairs so far found.

D. The temperature effect on the intercepts ID_1 (Table 4) is substantial. From 133 to 295 K the values $ID_1 \times 10^3$ drop from 67 to 20. As these values are representative for the yield of solvent separated ion pairs (eq 12), this means that the IP yield strongly reduces toward room temperature.

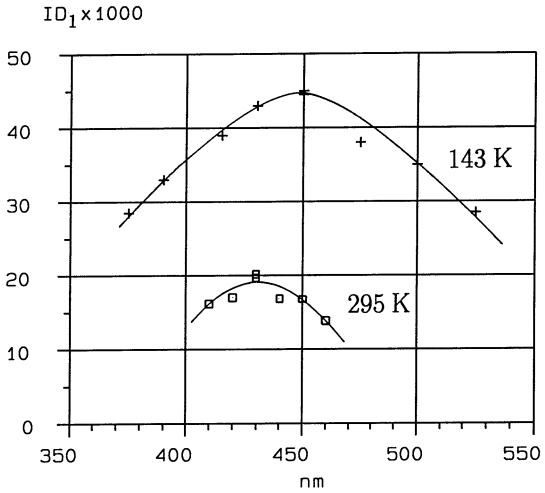

Figure 5. Pentachloroethane: Intercept spectra ID_1 for Penta in MCH at 143 and 295 K, normalized to 100 Gy (compare with the late λ_{max} in Table 1).

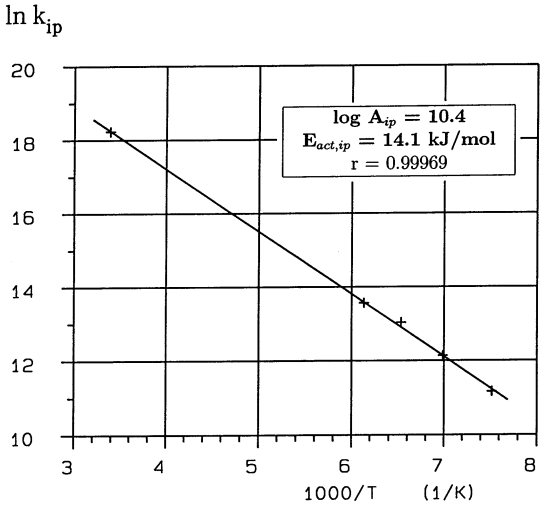

Figure 6. Pentachloroethane: Arrhenius plot for the rate constant k_{ip} (decay of the solvent separated ion pair, IP), including the Arrhenius parameters. The actual rate data are given in Table 4.

E. Detailed Analysis of Slope SD_1 and Intercept ID_1 allows us to improve on this qualitative conclusion. With eq 11 the product absorption coefficient $\epsilon_{pb} = \eta_b \times \epsilon_{ip}$ (the index b stands for MCH^+) may be calculated from the slope, and then with eq 12 the total scavenged anion yield G_{tot} may be derived from the intercept. The calculation is based on the fact that all absorption coefficients (ϵ_B^+, ϵ_C^+, ϵ^-, and ϵ_{ip}) are temperature

TABLE 5: Pentachloroethane (0.1 M): Absorption Coefficient $\eta_b(MCH^+)\epsilon_{ip}$ and the Total Scavenging Yield G_{tot} as Derived from Slopes SD_1 and Intercepts ID_1 (Table 4) by Eqs 11 and 12

	data used for the calculations[d]					result		for comparison
temp K	G_{fi} [6] $(100\ eV)^{-1}$	$(lf)/10^{-5}$ (eq 7)[a]	$f_b(MCH^+) = 1 - f_c(MCHene^+)$	β [6] $\mu s^{0.6}$	γ [5] $\mu s^{0.6}$	$\eta_b(MCH^+)\epsilon_{ip}$ [f] $(M^{-1}\ cm^{-1})$	G_{tot} $(100\ eV)^{-1}$	D_{fast}/D_{diff} [6,e]
133	0.06	1.84	0.87	4.5	26 [5,b]	3250	1.2	410
143	0.06	1.80	0.87	3.0	15.7	2550	1.3	186
153	0.06	1.76	0.87	2.0	6.2	1580	1.6	103
163	0.06	1.72	0.87	1.5 [4,b]	4.6 [4,b]	660	2.8	
295	0.12	1.54	1 [c]	0.145		500	2.3	10

[a] For 100 Gy and MCH density.[21] [b] Interpolated. [c] Estimated. [d] $\eta_c(MCHene^+) \approx 0$ (see Discussion). [e] D_{fast} is the mobility of the high mobility cation in MCH. [f] Is measure for η because ϵ_{ip} has much less variation.[25]

TABLE 6: Comparison of the Systems at 143 K, Listed with Increasing Anion Lifetime τ^- as Shown in Figure 7: Data for the Solute Anion (A^-), the Solvent Separated Ion Pair (IP), and the Final Pair of Geminate Ions (Normalized to 100 Gy)

MCH solutions		anion decay			IP yield	IP decay		final geminate line ($Solv^+ + Cl^-$)			
solute	conc M	k^- s^{-1}	τ^-	$AP^-(5\%)$ [20] $\mu s^{-0.6}$	$ID_1/10^{-3}$ (λ_{max})	k_{ip} s^{-1}	τ_{ip} μs	$Solv^+$	fraction MCH^+	δ_2 $\mu s^{-0.6}$	$ID_2/10^{-3}$
CCl_4 [1]	0.2	~ 10 [15]	~fs [c]	$\sim 10^5$	140 (470 nm)	9×10^3	111	MCH^+	100%	3.0	2.0
Penta [a]	0.1	$\sim 7 \times 10^6$	~150 ns	1.6	51 (450 nm)	1.9×10^5	5.3	MCH^+/ene^+	87% [e]	5.0 [e]	2.0
Hexa [a]	0.05	4.0×10^6	250 ns	1.15	36 (420 nm)	4.4×10^4	22.7	MCH^+/ene^+	87% [e]	5.0 [e]	2.0
$CHCl_3$ [5]	0.3	3.6×10^6	280 ns	1.1			$\ll\tau^-$ [d]	MCH^+/ene^+	51%	9.7	2.7
Tetra [19,b]	0.2	7.3×10^4	13.7 μs	0.1				MCH^+/ene^+	87%	5.0	2.0

[a] This paper. [b] 1112-Tetra. [c] Expected to dissociate within a vibrational period. [d] $\tau_{ip} \ll 280$ ns estimated (see text). [e] Assumed identical to the result for Tetra.

independent, except for a small variation of ϵ_{ip}.[25] Other values used are given in Table 5, together with the resulting data.

In the temperature range from 133 to 295 K, **the values for $\eta_b(MCH^+) \times \epsilon_{ip}$** drop from 3250 to 500. As the possible variation of ϵ_{ip} in this temperature range is much smaller, these values are representative for η_b, the efficiency for charge transfer from MCH^+ to $R^\bullet$ to yield ion pairs IP. It is important to see that this drop by a factor of about 6 correlates with the values for D_{fast}/D_{diff},[6] the ratio of the high mobility of the solvent cation to the diffusional mobility, as derived previously for MCH[6] (Table 5). This ratio drops by a factor of 40 for the same temperature range. In other words, the high mobility of MCH^+ (D_{fast}) drastically slows down relative to the diffusional mobility (D_{diff}) toward room temperature. Therefore, the drop of the efficiency η correlates with the cation mobility. It is concluded that the high mobility of the solvent cation is a requirement for positive charge transfer from MCH^+ to $R^\bullet$. This mechanism gains importance at very low temperatures; however, it loses importance at room temperature.

The total scavenging yield G_{tot} for $e_{solv} + RCl \rightarrow RCl^-$ is also given in Table 5. It indicates some increase with temperature. However, the accuracy is not high, and the mechanistic details of temperature dependences are not clear.

VII. Tetrachloroethane (Tetra)

A. A $t^{-0.6}$ plot of the rate curve for Tetra in MCH at 143 K looks different than the corresponding plots for Hexa and Penta (see comparison in Figure 7). There is no obvious saddle or plateau, which could imply a geminate line with high intercept and low slope. If one tries to fit a geminate line to the nearly linear portion at $t^{-0.6} \gtrsim 1.8\ \mu s^{-0.6}$, it has a high intercept. However, it then is impossible to find a fit for the first-order decay at $t^{-0.6} \lesssim 1.6\ \mu s^{-0.6}$. The rate curve is rather comparable with the $t^{-0.6}$ plot for $CHCl_3$ in MCH [5] (Figure 7). This means that the early part ($t^{-0.6} \gtrsim 0.8\ \mu s^{-0.6}$) is governed by the cationic mechanism (positive side in Scheme 3), whereas the late part corresponds to the $Tetra^-$ fragmentation (negative side in Scheme 1). Details of the simulation are given in the adjacent paper on Tetra[19] with its Scheme 1 and Figure 2.

TABLE 7: Solvent Separated Ion Pairs $(R^+|Solv|Cl^-)_{Solv}$ So Far Identified in Liquid Solutions

solvent separated IPs[a]	solution	references
$(CCl_3^+\|CCl_4\|Cl^-)_{CCl_4}$ [b]	neat CCl_4	22, 23
$(CCl_3^+\|MCH\|Cl^-)_{MCH}$	CCl_4 in MCH	2, 3
$(CCl_3^+\|Freon\|Cl^-)_{Freon\text{-}113}$ [c]	CCl_4 in Freon-113[d]	24
$((CH_3)_3C^+\|IO\|Cl^-)_{IO}$ [b]	CCl_4 in isooctane (IO)	3
$(CFCl_2^+\|MCH\|Cl^-)_{MCH}$	$CFCl_3$ in MCH	4
$(C_2Cl_5^+\|MCH\|Cl^-)_{MCH}$	Hexa in MCH	this paper
$(C_2HCl_4^+\|MCH\|Cl^-)_{MCH}$	Penta in MCH	this paper

[a] The transient absorption is always due to the CT band of $(R^+\cdot Solv)$; at high solute concentrations contribution from $(R^+\cdot Solute)$ is possible.[2] [b] R^+ is formed from $Solv^+$ fragmentation. [c] CCl_3^+ is formed from direct charge transfer: $Freon^+ + CCl_4 \rightarrow CCl_4^+ \rightarrow CCl_3^+$. [d] Freon-113 = $CFCl_2CF_2Cl$.

B. The anion fragmentation rate for **1112-Tetra** is $k^-(143\ K) = (7.3 \pm 0.6) \times 10^4\ s^{-1}$ with $E_{act} = 17.8$ kJ/mol and $\log A = 11.2$. For 1122-Tetra it is $k^-(143\ K) = (5.0 \pm 1.0) \times 10^4\ s^{-1}$ with $E_{act} = 16.9$ kJ/mol and $\log A = 10.9$.

VIII. Discussion: Survey and Comparison

A. With the three new solutes we have found support for the expected correlation of the formation of solvent separated ion pairs ($Solv^+ + R\cdot\cdot\cdot Cl^- \rightarrow IP$) with the anion lifetime τ^-. With τ^- of 150 ns ($Penta^-$) or 250 ns ($Hexa^-$) ion pairs are effectively produced, whereas with $\tau^- = 13.7\ \mu s$ ($Tetra^-$) they are not observed. The larger τ^-, the less likely ion pairs are formed. However, the anion lifetime is not the only criterion (see below).

B. An overview over the three new solutes, together with the two reference molecules CCl_4 and $CHCl_3$, is shown in Figure 7 with their typical rate curves at 143 K, arranged with increasing anion lifetimes τ^-. The major results from the various studies are marked in Figure 7 for quick comparison. The data are summarized in Table 6.

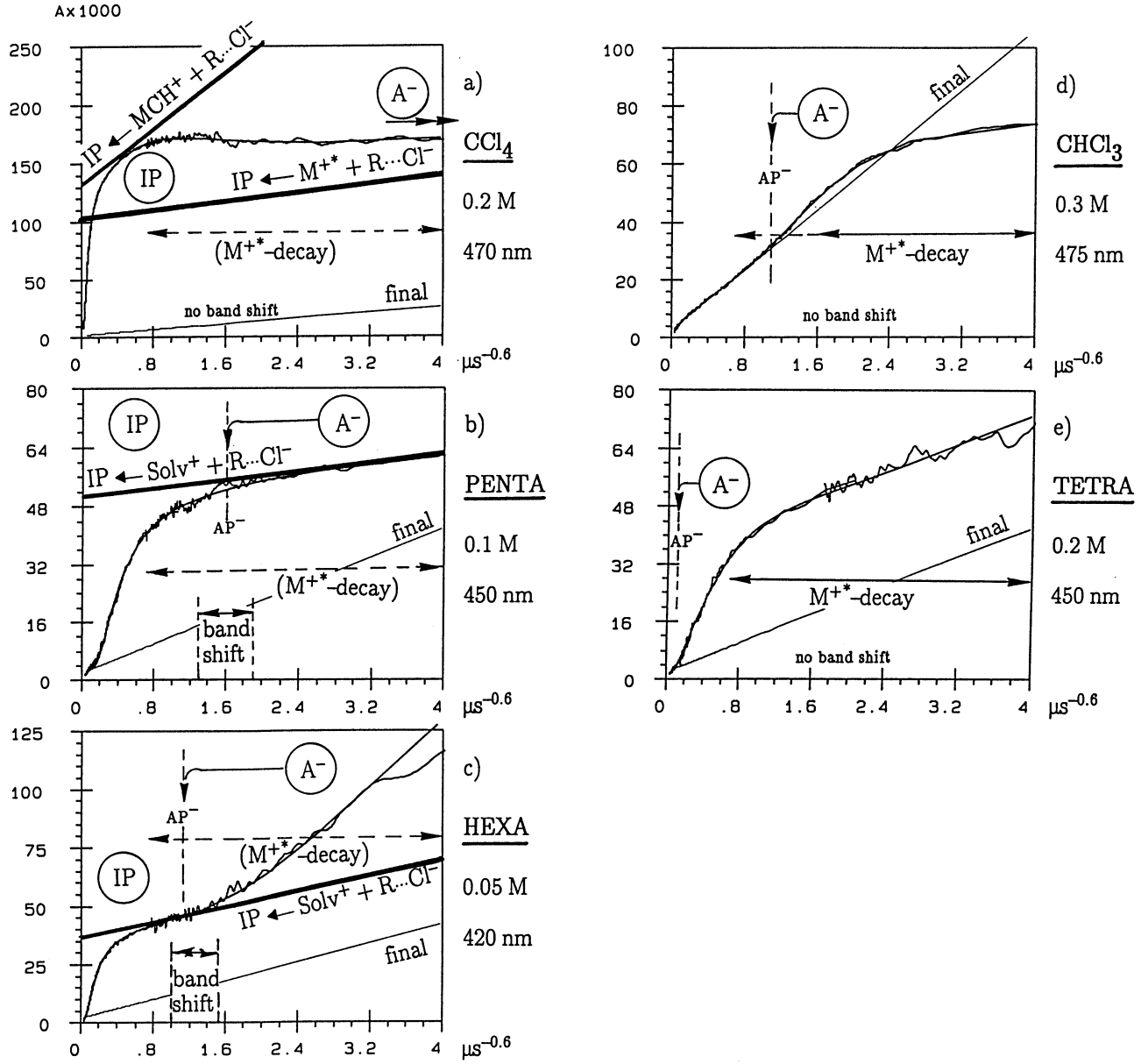

Figure 7. Comparison of the $t^{-0.6}$ plots of the geminate ion kinetics for CCl_4,[1] Penta, Hexa, $CHCl_3$,[5] and 1112-Tetra[19] at 143 K (normalized to 100 Gy), in the sequence of increasing anion lifetime τ^- (see Table 6). The major characteristics are marked as follows: *heavy lines*, the geminate lines leading to IP formation; *A^- decay*, in the region until AP^-(5%);[20] *IP decay*, if any, in the region after AP^-(5%);[20] *region of spectral band shift*, if any, *region of influence from the cationic mechanism "M^{+}* decay"*, dashed if hidden, full line if dominant (horizontal lines with arrows); *thin lines*, final geminate line for $Solv^+ + Cl^-$ (slope mainly influenced by the mobility values δ_2 (Table 6)).

SCHEME 4

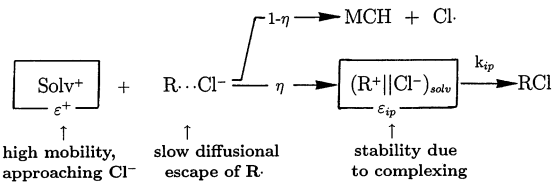

C. With Hexa and Penta there are two new examples with geminate ion recombination lines in $t^{-0.6}$ plots having high intercepts, which are due to the formation of solvent separated ion pairs, a product with optical absorption. In most cases known (Table 7) the solvent separated ion pairs are products in a characteristic geminate ion recombination, as illustrated in Scheme 4.

The solvent high mobility cation $Solv^+$ (M^{+*} or MCH^+) approaches with high speed the negative charge in the fragment pair ($R\cdot\cdot\cdot Cl^-$). Yet, this pair separates only by slow diffusional motion. Therefore, the high speed solvent cation may meet the fragment radical $R^\bullet$ before recombining with Cl^-. The result is positive charge transfer from $Solv^+$ to $R^\bullet$ to yield R^+, which immediately complexes with the solvent. As this charge-transfer process occurs in the direct neighborhood of Cl^-, the immediately following recombination with Cl^- leads to a solvent separated ion pair,[2] instead of to a straight neutralization. We have previously shown that the characteristics of the absorption band are compatible with the assignment to the CT band ($R^+ \leftarrow MCH$).[2,4] It therefore serves as a label within the solvent separated ion pair and follows its decay. Complexing is at the same time reason for the stability of the solvent separated ion pairs (IP).

D. The efficiency η for positive charge transfer (Scheme 4) is introduced, as only a fraction of all solvent cations may lead to charge transfer to the radical R•.

1. There is a steric condition: obviously R must be on the proper side of Cl^-, which means near the line of approach of the positive charge (between $Solv^+$ and Cl^-).

2. There is a competition between the mobilities of the cation (D_{fast}) approaching Cl^- and the diffusional escape of R• (D_{diff}) out of the Coulombic region. Therefore, the mobility D_{fast} must be larger than D_{diff} to overcome the radical escape. $D_{fast}/D_{diff} \gg 1$ is the condition for effective charge transfer.

(a) For Penta the correlation of η with D_{fast}/D_{diff} has been documented in Table 5. In the temperature range from 133 to 295 K, η was found to decrease by a factor of about 6, parallel to D_{fast}/D_{diff} decreasing from 410 to 10. This implies that the mechanism of charge transfer to R• loses importance toward room temperature.

(b) For the fragment cation $MCHene^+$ the mobility is D_{diff}. It is therefore highly unlikely that $MCHene^+$ may contribute to the IP production ($\eta_c(MCHene^+) \approx 0$).

3. The geminate pairs of ions (on ionization) cover a large range of initial separations. Correspondingly, the high mobility cations arrive at different times at ($R\cdot\cdot\cdot Cl^-$), earlier if they started at shorter distance, later at long distance. Early means higher efficiency η; later means lower η. The efficiency η is time dependent! Experimentally only a mean value is accessible, weighed by the distribution function of initial ion pair separations (shorter distances dominate strongly).

E. The charge-transfer process from $Solv^+$ to R• is only possible if the ionization potential $I_p(R•)$ is smaller than $I_p(MCH) = 9.85$ eV.[26] The I_p values for CCl_3• and $CHCl_2$• are 8.78 and 9.3 eV, respectively, permitting positive charge transfer. For the other radicals the $I_p(R)$ values are not known. However, it is concluded that the R groups from $Penta^-$ and $Hexa^-$ must also have $I_p(R•) < 9.85$ eV (MCH), as ion pairs are formed. For $CHCl_3$, charge transfer to $CHCl_2$• should obviously be possible. The reasons that it cannot be observed are discussed below.

For the three isomers of $MCHene^+$, I_p values are known to be between 8.67 and 8.94 eV.[26] Therefore, charge transfer from $MCHene^+$ to R• is not possible or is unlikely. The previous finding that its mobility is too low (see above) now finds an additional argument against charge transfer.

F. Yields of Solvent Separated Ion Pairs (IP). In eq 12 the second term with G_{tot} dominates ($G_{tot} \gg G_{fi}$) and $\epsilon_{pc} \approx 0$, because $\eta_c(MCHene^+) \approx 0$ (see above). Therefore, the intercept $IX \approx G_{tot}(lf)f_b\eta_b\epsilon_{ip}$ is a measure for the IP yield, as already argued for ID_1 in section VI on Penta. Table 6 shows a strong reduction of this value with increasing anion lifetime, with the yield for CCl_4 being highest. Obviously, comparing the intercepts means ignoring the dependence of $\epsilon_{ip}(R^+\cdot MCH)$ on R and the dependence of G_{tot} on the solute concentrations. However, the general trend fits the expectation: the later R becomes available for charge transfer, the lower the efficiency η_b.

G. If no ion pairs are detectable, as for $CHCl_3$ and Tetra, there are several possible reasons, listed here in the order of declining importance:

1. The anion lifetime τ^- may be too long and the availability of R for charge transfer too late, which means $\eta \rightarrow 0$.

2. The ion pair lifetime τ_{ip} may be much shorter than the rate of its production (which means $\tau_{ip} \ll \tau^-$). IPs may be formed yet cannot be seen.

3. The absorption coefficient of the ion pair $\epsilon_{ip}(R^+\cdot MCH)$ may be *too low* (or the absorption is outside of the experimental λ range). However, such CT bands are typically strong and are often in the visible λ range.

4. The condition for the ionization potentials, $I_p(R) < I_p(MCH)$, is not met (see above).

For Tetra, argument 1 is the most likely one (τ^- too long). For $CHCl_3$, where $\tau^-(CHCl_3^-)$ is near $\tau^-(Hexa^-)$, argument 2 is more likely (decay faster than its buildup rate). This would mean that, for $CHCl_3$, $\tau_{ip} \ll 280$ ns (τ^-).

Acknowledgment. Support by the Swiss National Science Foundation and by the Research Funds of ETH-Zürich is gratefully acknowledged.

References and Notes

(1) Bühler, R. E. *Radiat. Phys. Chem.* **2001**, *60*, 323.
(2) Gebicki, J. L.; Domazou, A. S.; Ha, T.-K.; Cirelli, G.; Bühler, R. E. *J. Phys. Chem.* **1994**, *98*, 9570.
(3) Gremlich, H.-U.; Bühler, R. E. *J. Phys. Chem.* **1983**, *87*, 3267.
(4) Domazou, A. S.; Quadir, M. A.; Bühler, R. E. *J. Phys. Chem.* **1994**, *98*, 2877.
(5) Bühler, R. E.; Domazou, A. S.; Katsumura, Y. *J. Phys. Chem. A* **1999**, *103*, 4986.
(6) Katsumura, Y.; Azuma, T.; Quadir, M. A.; Domazou, A. S.; Bühler, R. E. *J. Phys. Chem.* **1995**, *99*, 12814.
(7) Bühler, R. E.; Katsumura, Y. *J. Phys. Chem.* **1998**, *102*, 111.
(8) Jto, Y.; Tabata, Y. Single particle pulse radiolysis. In *Pulse Radiolysis*; Tabata, Y., Ed.; CRC Press: Boca Raton, FL, 1991; p 237.
(9) Bühler, R. E. *Res. Chem. Intermed.* **1999**, *25*, 259. Due to printing errors, ask the author for a corrected reprint.
(10) Hurni, B.; Brühlmann, U.; Bühler, R. E. *Radiat. Phys. Chem.* **1975**, *7*, 499.
(11) Kobayashi, H.; Ueda, T.; Kobayashi, T.; Washio, M.; Tabata, Y. *Radiat. Phys. Chem.* **1983**, *21*, 13.
(12) Schuler, R. H.; Patterson, L. K.; Janata, E. *J. Phys. Chem.* **1980**, *84*, 2088.
(13) van den Ende, C. A. M.; Warman, J.; Hummel, A. *Radiat. Phys. Chem.* **1984**, *23*, 55.
(14) Bartczak, W. M.; Hummel, A. *Radiat. Phys. Chem.* **1994**, *44*, 335.
(15) Bartczak, W. M.; Hummel, A. *Radiat. Phys. Chem.* **1997**, *49*, 675.
(16) Bühler, R. E. *Can. J. Phys.* **1990**, *68*, 918.
(17) Bühler, R. E.; Quadir, M. A. *J. Phys. Chem. A* **1999**, *104*, 2634.
(18) Bühler, R. E. *Proc. Trombay Symposium on Radiation and Photochemistry TSRP 98*, BARC, Trombay, Mumbai, India, Jan 14−19, 1998; Part II, p 429.
(19) Bühler, R. E.; Quadir, M. A. *J. Phys. Chem. A* **2003**, *107*, 11354.
(20) Due to time compression toward late times in $t^{-0.6}$ plots, the "end" of a reaction corresponds to an easily recognizable point, called the "anchor point" (AP) for the particular reaction.[9] It is usually calculated for 99% completion of the reaction (1% rest) by $AP = x(k_1 \times 10^{-6})^{0.6}\ \mu s^{-0.6}$ with $x = 0.4$. For 5% rest, AP(5%) has $x \approx 0.5$, and for 10% rest, AP(10%) has $x \approx 0.6$.
(21) Quadir, M. A. Geminate Ion Kinetics in Alkane Solvents, Studied by Pulse Radiolysis. Thesis ETH No. 11075, 1995.
(22) Bühler, R. E. *Radiat. Phys. Chem.* **1983**, *21*, 139.
(23) Bühler, R. E.; Hurni, B. *Helv. Chim. Acta* **1978**, *61*, 90.
(24) Hurni, B.; Bühler, R. E. *Radiat. Phys. Chem.* **1980**, *15*, 231.
(25) In the temperature range 113 K to 293 K, ϵ_{ip} (for a charge-transfer band) may vary up to 40% (see: Briegleb, G. *EDA-Komplexe*; Springer: 1961; p 69).
(26) *Handbook of Chemistry and Physics*; CRC Press Inc.: Boca Raton, FL, 1983.